Extended Abstracts of the 2019 International Conference on Solid State Devices and Materials, Nagoya, 2019, pp905-906

New Contact-first Two-dimensional Transistor

Yu-Wei Kang[1, *], Chun-Jung Su[2, **] and Tuo-Hung Hou[1, 3]

[1] International College of Semiconductor Technology, National Chiao-Tung University, Hsinchu, Taiwan
[2] Taiwan Semiconductor Research Institute, Hsinchu, Taiwan
[3] Department of Electronics Engineering, National Chiao-Tung University, Hsinchu, Taiwan
*Tel: +886-3-5712121#54219; E-mail: ywkang.ep02@g2.nctu.edu.tw
**Tel: +886-3-5726100; E-mail: cjsu@narlabs.org.tw

Abstract

We propose and demonstrate a contact-first integration scheme for fabricating two-dimensional (2D) field-effect transistors. Utilizing this new scheme, two orders of magnitude improvement in the on-current is achieved in MoS_2 devices with robust process yields. We carefully verify that this scheme prevents the damage from the developer chemical during the lithography process. We also show that this process can be applied for other 2D materials as well, such as large-area PVD-synthesized $MoTe_2$.

1. Introduction

Two-dimensional transition metal dichalcogenide (TMD) devices have been widely investigated since the first MoS_2 transistor [1] was successfully demonstrated. That is because the TMD materials possess several unique characteristics, such as atomic thickness with desirable mobility and good immunity to short channel effects. However, 2D materials are easily peeled off during the fabrication process because of the weak interaction with the substrates. In addition, chemicals in the lithography process might also damage the 2D materials substantially. In this study, we propose a new contact-first process integration scheme to avoid the aforementioned concerns, thus achieving better device performance and yield. To prove the concept, we demonstrated the contact-first monolayer (ML) MoS_2 and also PVD-synthesized $MoTe_2$ [2] transistors.

2. Experiment Procedures

Figs. 1 (a) and (b) depict the device structures and process flows of both contact-first and conventional contact-last MoS_2 transistors, respectively. Compared to the conventional contact-last devices, the formation of source and drain metal (Mo) of the contact-first structure was performed before the ML-MoS_2 transfer [3]. The ML-MoS_2 was synthesized by chemical vapor deposition (CVD) on sapphire substrates [4]. To improve the device stability in air, a 20 nm-thick E-gun SiO_2 capping was deposited on both device structures [5]. Lastly, the active regions were patterned by HDP-RIE.

3. Result and Discussion

Figs. 2 (a) and (b) show the OM images of contact-first and contact-last MoS_2 devices after the S/D metal lift-off process, respectively. Severe MoS_2 peeling appeared in the contact-last devices as shown in Fig. 2(b), while well-defined patterns were found in the contact-first devices (Fig. 2(a)). Fig. 3(a) depicts the transfer curves (I_D-V_G) for the contact-first versus conventional contact-last devices. The on-current of the contact-first device increases almost two orders of magnitude. Furthermore, a notable improvement of mobility was also found in Fig. 3(b). The degradation in the conventional contact-last devices could be attributed to either the difference in the structure or the difference in the lithography process. To clarify this effect, the contact-first structure was used. To mimic the lithography process of the contact-last devices, one of the devices in Fig. 4 was fabricated with photoresist (PR) coating in direct contact with the MoS_2 channel. Fig. 4 shows comparable device performance for the MoS_2 devices in contact with PR and SiO_2 capping, which suggests no adverse impacts induced by PR. Secondly, to further investigate the effect of the developer, we compared two identical structures, in which one of the MoS_2 films was immersed in the Tetramethylammonium Hydroxide developer, which is commonly used in near ultra-violet positive photoresist development, before it was transferred. The I_D-V_G curves in Fig. 5 confirm that MoS_2 is substantially damaged by the developer. Such degradation was also observed from the OM and PL spectroscopy in Fig. 6. By comparison, the red and black circles in Figs. 6 (a) and (b) indicate that the grain boundary of two triangle-shaped MoS_2 was etched by the developer.

To prove the generality of the contact-first structure, we applied it to large-area PVD-synthesized $MoTe_2$. Fig. 7(a) is the Raman spectroscopy of the $MoTe_2$ after transfer. The I_D-V_G curve of contact-first $MoTe_2$ device is shown in Fig. 7(b). Fig. 7(c) illustrates the cross-sectional TEM image of the contact-first structure. The $MoTe_2$ was able to be transferred conformally onto the Pd electrodes and perfectly adheres to Pd and the substrate.

4. Conclusions

The contact-first structure not only alleviates the poor yield of the metal lift-off process on 2D materials but also avoids degradation induced by developer etching. We successfully demonstrated contact-first structures on monolayer MoS_2 and multilayer $MoTe_2$. The device performance shows enhanced I_{ON} and smaller deviation compared to the conventional contact-last counterpart. Thus, the contact-first structure is promising to achieve ideal van der Waals contact, which can approach the Schottky-Mott limit similar to the transfer metal techniques [6, 7].

Acknowledgements

This work was supported by the Ministry of Science and Technology, Taiwan, under Grant MOST-107-2628-E-492-001-MY3, 108-2633-E-009-001 and 108-3017-F-009-003. And in part supported by the "Center for Semiconductor Technology Research" from the Featured Areas Research Center Program within the framework of the Higher Education Sprout Project by the Ministry of Education (MOE) in Taiwan.

References

[1] B. Radisavljevic et al., *Nat. Nanotech.*, **6**, 147 (2011). [2] J. H. Huang et al., *Adv. Mater. Interfaces*, **4**, 1700157 (2017). [3] A. Gurarslan et al., *ACS Nano*, **8**, 11522 (2014). [4] C. P. Lin et al. *SSDM*, B-4-4 (2015) [5] D. J. Late et al., *ACS Nano*, **6**, 5635 (2012). [6] Y. Liu et al., *Nature*, **557**, 696 (2018). [7] J. Wang et al., *IEDM*, 22.3.1-22.3.4 (2018)

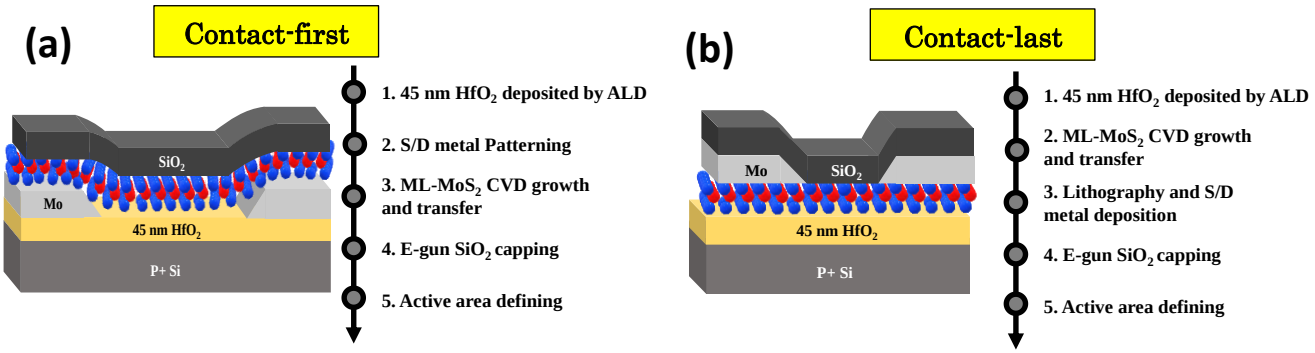

Fig. 1 Process flow and device structure of (a) the contact-first device and (b) the typical contact-last device. The thickness of E-gun SiO_2 is 20 nm.

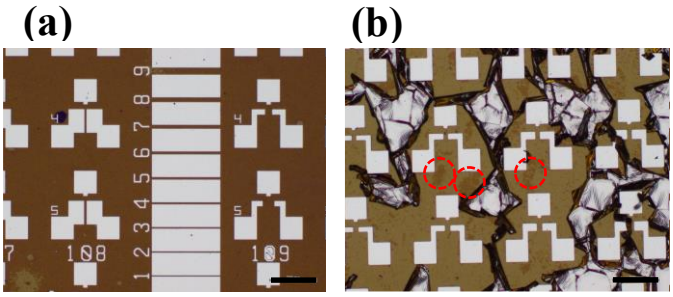

Fig. 2 Optical images of (a) the contact-first devices exhibit the intact MoS_2 film after process, (b) the contact-last devices reveal severe peeling of MoS_2 during the S/D metal lift-off process. The red circles indicate the remaining MoS_2 on the substrate. Scale bars are 200 μm.

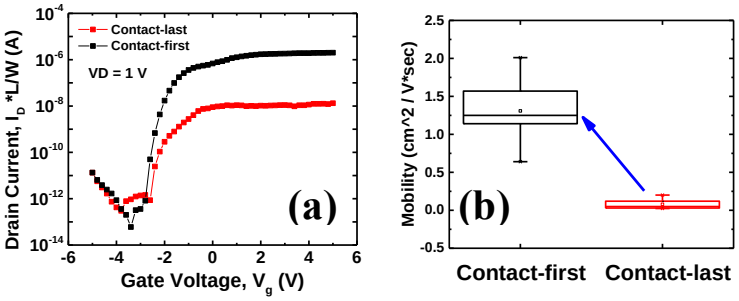

Fig. 3 (a) Transfer curves of contact-first and contact-last devices measured at V_D = 1V. (b) The mobility was extracted from the same specimens in (a).

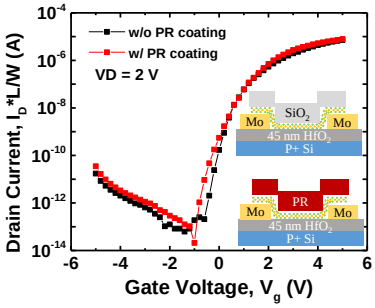

Fig. 4 I_D-V_G curves of the contact-first devices indicate comparable performance regardless of PR or SiO_2 in contact with the MoS_2.

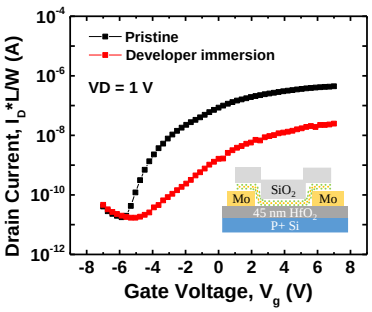

Fig. 5 I_D-V_G curves show the device performance degrades once the MoS_2 is exposed to the developer. Inset illustrates the device structure.

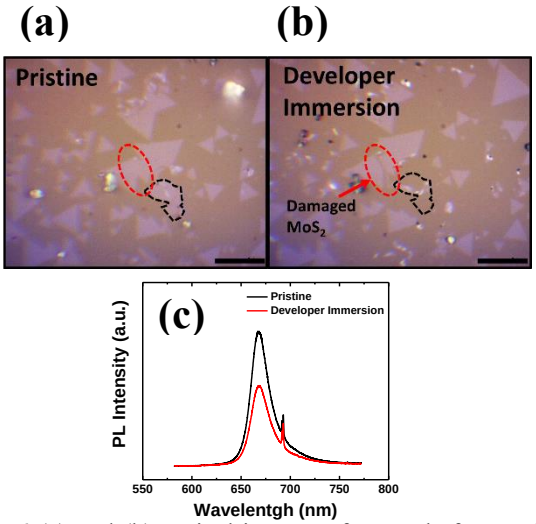

Fig. 6 (a) and (b) optical images of MoS_2 before and after being immersed in the developer. The red and black regions reveal the damaged MoS_2 after developer immersion. (c) The PL spectroscopy also indicates the degradation on the remaining MoS_2 after dipping in the developer. Scale bars are 20 μm.

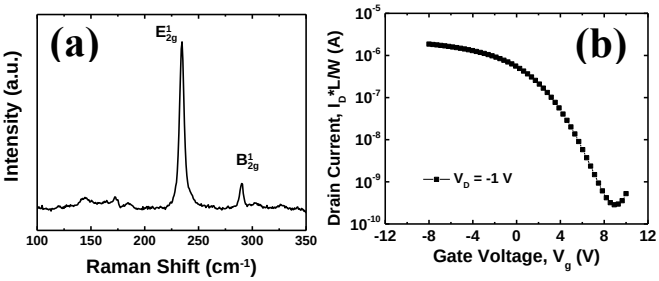

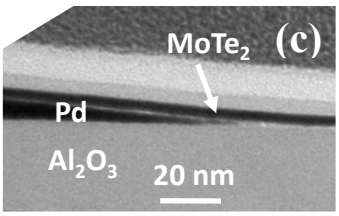

Fig. 7 (a) Raman spectroscopy of $MoTe_2$ after transfer. (b) Transfer curve of $MoTe_2$ was measured at V_D = -1V. (c) Cross-sectional TEM image of a PVD-synthesized 2H-$MoTe_2$ device with 4 μm channel length.